

Article

Numerical Assessments of Leaf Area Index in Tropical Savanna Rangelands, South Africa Using Landsat 8 OLI Derived Metrics and In-Situ Measurements

Timothy Dube ^{1,*}, Santa Pandit ², Cletah Shoko ³, Abel Ramoelo ^{4,5}, Dominic Mazvimavi ¹ and Tatenda Dalu ⁶

¹ Department of Earth Sciences, University of the Western Cape, Private Bag X17, Bellville 7535, South Africa; dmazvimavi@uwc.ac.za

² Graduate School of Agricultural and Life Sciences, University of Tokyo, 1-1-1 Yayoi, Bunkyo-Ku, Tokyo 113-8567, Japan; pandit-santa27@g.ecc.u-tokyo.ac.jp

³ School of Geography, Archaeology and Environmental Studies, University of Witwatersrand, Private Bag 3, Johannesburg 2050, South Africa; cletah.shoko@wits.ac.za

⁴ South African National Parks, P.O. Box 787, Pretoria 0001, South Africa; abel.ramoelo@gmail.com

⁵ Risk and Vulnerability Center, University of Limpopo, P Bag X1106, Sovenga 0727, South Africa

⁶ Department of Ecology and Resource Management, University of Venda, Private Bag X5050, Thohoyandou 0950, South Africa; dalutatenda@yahoo.co.uk

* Correspondence: tidube@uwc.ac.za; Tel.: +27-21-959-4130

Received: 20 February 2019; Accepted: 2 April 2019; Published: 7 April 2019



Abstract: Knowledge on rangeland condition, productivity patterns and possible thresholds of potential concern, as well as the escalation of risks in the face of climate change and variability over savanna grasslands is essential for wildlife/livestock management purposes. The estimation of leaf area index (LAI) in tropical savanna ecosystems is therefore fundamental for the proper planning and management of this natural capital. In this study, we assess the spatio-temporal seasonal LAI dynamics (dry and wet seasons) as a proxy for rangeland condition and productivity in the Kruger National Park (KNP), South Africa. The 30 m Landsat 8 Operational Land Imager (OLI) spectral bands, derived vegetation indices and a non-parametric approach (i.e., random forest, RF) were used to assess dry and wet season LAI condition and variability in the KNP. The results showed that RF optimization enhanced the model performance in estimating LAI. Moderately high accuracies were observed for the dry season (R^2 of 0.63–0.72 and average RMSE of $0.60 \text{ m}^2/\text{m}^2$) and wet season (0.62 – 0.63 and $0.79 \text{ m}^2/\text{m}^2$). Derived thematic maps demonstrated that the park had high LAI estimates during the wet season when compared to the dry season. On average, LAI estimates ranged between 3 and $7 \text{ m}^2/\text{m}^2$ during the wet season, whereas for the dry season most parts of the park had LAI estimates ranging between 0.00 and $3.5 \text{ m}^2/\text{m}^2$. The findings indicate that Kruger National Park had high levels of productivity during the wet season monitoring period. Overall, this work shows the unique potential of Landsat 8-derived metrics in assessing LAI as a proxy for tropical savanna rangelands productivity. The result is relevant for wildlife management and habitat assessment and monitoring.

Keywords: climate variability; natural capital; rangeland productivity; seasonal variability; wildlife

1. Introduction

Savanna ecosystems comprise socio-economically and ecologically important biodiversity resources. These ecosystems consist of grasses, scattered forests and shrubs, which provide wildlife and livestock with grazing resources as well as other ecosystem goods and services. Most rural communities

around tropical savanna ecosystems practice wildlife hunting to sustain their livelihoods [1]. Therefore, continuous monitoring of these ecosystems is crucial as they are key natural capital or resources. So far, productivity in these ecosystems is more often assessed using two plant biophysical properties, which are the leaf area index (LAI) and aboveground biomass (AGB) [2]. These parameters play a major role in animal productivity and can help provide insights on rangelands condition, in terms of the quality and quantity of natural capital. Besides, they indirectly sustain livelihoods. For example, when forage is high in terms of quantity and quality, there will be an increase in livestock productivity, thus leading to less importation and more exports of beef products in the country. Ecosystems that are healthy and highly productive play an important role in the country's economy, through wildlife production and livestock grazing enhancement and tourism [3].

The presence of vast amounts of forage resources is linked to wildlife productivity, and this can contribute to the economy through tourism, which accounts for about 9% of employment in South Africa [4]. Like any other rangeland type, tropical savanna ecosystems are compromised by the lack of proper operational assessment and monitoring frameworks in place. Hence, overgrazing, bush encroachment and land degradation are characteristic of a number of these ecosystems, particularly in the southern African region. For instance, towards the end of the dry season, most of the southern African countries within tropical savanna biomes lose a large number of wildlife and livestock populations annually due to rangelands degradation [1]. The area of land grazed by livestock is projected to decrease by almost 50% by 2050 in the sub-Saharan Africa savannas [5]. If sustainable, efficient and equitable use of these resources is to be achieved, it is important to understand the spatial and temporal dynamics of tropical savanna rangelands. For this reason, LAI monitoring is crucial.

LAI is an important variable for determining forage quantity within vegetated ecosystems, and by definition it is one-half of the total green leaf area per unit ground surface area of vegetation canopy. In the past, methods that were used to estimate LAI focused on LAI measurement strategy and theory, using litter fall collection and point quadrat sampling [6,7]. However, these methods are time-consuming and labour intensive. Historically, the LAI has been measured on crop canopies using in-situ (destructive) approaches. Although in-situ approaches are accurate and easy to implement, they have their own limitations: they are laborious and time-consuming, the sample-based measurements are spatially discontinuous, and they are difficult to operationalize and landscape scale [7]. Recently, Zheng and Moskal [6] highlighted appropriate methods for measuring LAI using remote sensing, which has the advantage of being dynamic and operational, with the ability to overcome challenges associated with the sparse nature of ground-based field measurements.

Further, a couple of studies have estimated or predicted LAI using remotely sensed data, and most of these were not linked to tropical savanna ecosystems or rangeland productivity. Those that focused on rangeland productivity focused on plot-level monitoring or used very coarse satellite data like MODIS or high-spatial-resolution data that are costly and spatially restricted [8–11]. For example, References [8,9] studied the spatial variation of ecosystem structure functions at a landscape scale in mountainous areas of Japan. Further, Cui and Kerekes [12] applied three retrieval approaches based on vegetation indices, physical model-based lookup table (LUT) inversion and machine learning to estimate LAI simulated from the SPectra bARrax Campaign (SPARC 2003) field campaign HyMap hyperspectral data. Although most of these studies reported high-accuracy LAI estimates, their approaches cannot be operationalised in extensive tropical savanna rangelands, given the cost of high-resolution data acquisition and the curse of dimensionality [13]. The medium-resolution Landsat 8 Operational Land Imager (OLI) sensor is one of the key primary data sources. It is highly suitable and practical for regional LAI analysis, especially in resource-limited areas. The Landsat 8 OLI, as a multispectral push-broom scanner, was designed to achieve high radiometric image resolution, with minimal signal-to-noise ratio. The sensor collects data in nine spectral bands, with a spatial resolution of 30 m in bands 1–7 and 9 [3]. It is therefore crucial to assess the advantage of increased radiometric resolution of Landsat 8 OLI on estimating LAI in tropical savanna rangelands [6].

Furthermore, the Landsat 8 OLI sensor provides (i) a refined spectral range for certain bands that have been found to be critical for improving the detection of subtle vegetation properties and spectral responses across the near-infrared (NIR) and panchromatic bands, and (ii) an improved radiometric resolution from 8 to 12 bits, which are critical in enabling the characterization of different forest conditions [7]. Landsat 8 OLI's high spatial resolution makes it ideal for vegetation mapping and monitoring applications. Findings from Landsat 8 OLI can help to conserve tropical savanna rangelands through the provision of accurate and up-to-date information about rangeland conditions and ecosystem dynamics, as well as changes in productivity in terms of quantity and quality. Such findings can help guide farmers, resource managers and land use planners with baseline information needed for developing sustainable rangeland management practices. Thus, the aim of this study was to assess the spatio-temporal seasonal dynamics in LAI, as a proxy for rangeland condition and productivity in the Kruger National Park, South Africa, using multispectral Landsat 8 OLI.

2. Materials and Methods

2.1. Study Area

The study was conducted in the protected Kruger National Park (KNP), which covers sections of the Limpopo and Mpumalanga provinces of South Africa (Figure 1). The park is characterized by arid to semi-arid savanna biome, with gentle slopes that make it suitable for wildlife grazing (Figure 2). The area has a humid subtropical climate, with cool-dry winters and hot-wet summers. Annual average rainfall ranges between 0 and 553 mm, with annual average summer and winter temperatures of 28 °C and 16 °C, respectively. The dry season stretches from mid-June to mid-November and the wet season ranges from mid-November to early July. The dominant vegetation cover in the area includes grasslands, mopane, marula and acacia trees, etc.

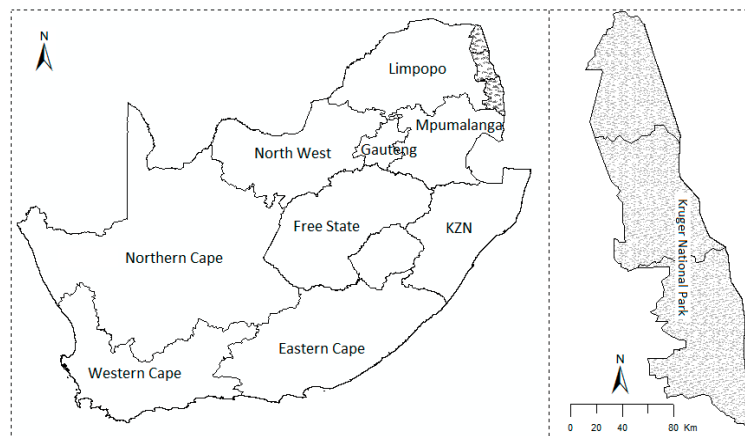


Figure 1. Location of the study area.



Figure 2. Typical landscapes found within the Kruger National Park.

2.2. LAI Field Measurements

LAI measurements were conducted across the Kruger National Park, South Africa. The Kruger National Park was considered for this study due to the high presence of wildlife grazing in the area as well as its economic value. Field data collection was done during the wet and dry seasons in 2016 and 2017. Sampling for the dry season was from 19 to 20 September 2016, with 74 plots being surveyed, whereas 195 plots were sampled during the wet season from 13 to 16 March 2017. Sampling plots were selected using a random sampling technique based on accessibility within the protected area. The coordinates for each sampled plot within the park were recorded using a handheld Global Positioning System (GPS). For LAI measurements, a LICOR 2200 plant canopy analyser was used under clear sky conditions (i.e., without clouds) to ensure that LAI was not underestimated. LAI measurements of each plot were obtained by calculating an average for LAI above canopy ($n > 3$) and below canopy ($n > 3$) measurements taken from each plot.

2.3. Satellite Acquisition and Pre-Processing

Landsat 8 OLI satellite images for the wet (12 September 2016) and dry (22 March 2017) season were acquired from the USGS Earth Explorer (<https://earthexplorer.usgs.gov/>). A detailed summary on the Landsat 8 satellite images used is provided in Table 1. Top of atmosphere (TOA) reflectance Landsat 8 OLI bands were considered. These bands encompass visible, Near Infra-Red (NIR), and Short Wave Infra-Red (SWIR) regions of the electromagnetic spectrum. TOA reflectances were atmospherically corrected using Landsat Ecosystem Disturbance Adaptive Processing Systems, which masks out clouds, shadows and water, among other non-target effects. As such, no further pre-processing was implemented. Spectral reflectances from Landsat 8 OLI images for different dates were then extracted corresponding to each leaf area index sample GPS location. The extracted spectral reflectances were then used to calculate selected vegetation indices. The most commonly used vegetation indices in obtaining the leaf characteristics of plants are shown in Table 2. In total, 21 remotely sensed variables were used to build a relationship with the field-measured LAI. The indices were chosen based on their performance as described in literature.

Table 1. Summary detail of the Landsat 8 OLI used for this work.

Season	Image Scene Detail	Date of Acquisition
Dry	LC08_L1TP_168077_20161022_20170319_01_T1	22 October 2016
	LC08_L1TP_169076_20161029_20170319_01_T1	29 October 2016
Wet	LC08_L1TP_168077_20170518_20170525_01_T1	18 May 2017
	LC08_L1TP_169076_20170525_20170614_01_T1	25 May 2017

Table 2. Spectral vegetation indices used in LAI retrieval. Abbreviations: NDVI: normalized difference vegetation index; SR: simple ratio; SAVI: soil adjusted vegetation index; EVI: enhanced vegetation index; EVI2: enhanced vegetation index—improved; PSRI: plant senescence reflectance index; CRI1: carotenoid reflectance index 1; GVI: green vegetation index; GNDVI: green normalized difference vegetation index; GCI: green chlorophyll index; MSR: modified simple ratio; ARVI: atmospherically resistant vegetation index; MCARI: modified chlorophyll absorption ratio index; MTVI2: modified triangular vegetation index—improved.

Vegetation Indices	Algorithm	Reference
NDVI	$\text{NIR} - \text{RED} / \text{NIR} + \text{RED}$	[8]
SR	NIR / RED	[9]
SAVI	$((\text{NIR} - \text{RED}) / (\text{NIR} + \text{R} + \text{L})) \times (1 + \text{L})$	[10]
EVI	$2.5 \times (\text{NIR} - \text{RED}) / (\text{NIR} + 6\text{RED} - 7.5 \times \text{BLUE} + 1)$	[11]
EVI2	$2.4 \times (\text{NIR} - \text{RED}) / (\text{NIR} + \text{RED} + 1)$	[11]
PSRI	$(\text{RED} - \text{GREEN}) / \text{NIR}$	[12]
CRI1	$(1 / \text{BLUE}) - (1 / \text{GREEN})$	[13]

Table 2. Cont.

Vegetation Indices	Algorithm	Reference
GVI	NIR/GREEN	[14]
GNDVI	$(\text{NIR} - \text{GREEN})/(\text{NIR} + \text{GREEN})$	[15]
GCI	$(\text{NIR}/\text{GREEN}) - 1$	[16]
MSR	$(\text{NIR}/\text{RED}) - 1/\sqrt{((\text{NIR}/\text{RED}))} + 1$	[17]
ARVI	$\text{NIR} - (\text{RED} - 1 \times (\text{BLUE} - \text{RED}))/\text{NIR} + (\text{RED} - 1 \times (\text{BLUE} - \text{RED}))$ where, $1 = \gamma$	[18]
MCARI	$1.5 \times (2.5 \times (\text{NIR} - \text{RED}) - 1.3 \times (\text{NIR} - \text{BLUE}))/\sqrt{((2 \times \text{NIR} + 1)^2 - (6 \times \text{NIR} - 5 \times \text{RED}) - 0.5)}$	[19]
MTVI2	$1.5 \times (1.2 \times (\text{NIR} - \text{GREEN}) - 2.5 \times (\text{RED} - \text{GREEN}))/\sqrt{((2 \times \text{NIR} + 1)^2 - (6 \times \text{NIR} - 5 \times \sqrt{(\text{RED}) - 0.5})}$	[20]

2.4. Random Forest Algorithm for LAI Estimates

The random forest (RF) regression technique was used to estimate and map dry and wet season LAI within Kruger National Park. RF has recently gained popularity in environmental and agricultural studies using remotely sensed data [21,22]. Its advantage is that it uses training samples to develop multiple nodes of the trees—a set of conditions which are applied from the roots to the leaves of the model trees and the results are averaged from each individual tree to better predict LAI [23]. In addition, the RF model for each tree was trained with independent bootstrap samples (i.e., two-thirds of samples), which were selected randomly from the sample data set. The remaining one-third of the data, which was not used in growing trees, is called the out-of-bag (OOB) data and was used for model validation [24]. The OOB data were further used to rank the variables based on their contribution to the model accuracy and are often expressed in percentage increased mean squared error (%IncMSE) and increased node purity (IncNodePurity) [21]. %IncMSE is the most robust and informative accuracy measure. It is the increase in MSE of predictions (estimated with out-of-bag-CV) as a result of a variable being permuted (values randomly shuffled). The IncNodePurity relates to the loss functions, which are chosen by best splits. The loss function is the MSE for regression and Gini-impurity for classification. Another advantage of the RF model is its tuning parameters, such as *ntrees* (number of trees used in a model), *mtry* (number of variables available for splitting at each node of the tree) and node size (at each terminal node of an individual tree containing a fixed pre-specified number of observations). The default value for *ntree* was 500, *mtry* was one-third of the total number of variables, and node size values ranged from 1 to 5 [25]. Further, variable screening was done using the backward elimination of the least-important variables generated from the OOB data to determine the most important variables for LAI estimation. Previous studies have demonstrated that variable screening is important as it helps to strengthen the model performance by eliminating the weak variables in model building [14–16]. Houborg and McCabe [14] argue that the development and application of machine-learning methods should be carefully guided by prior “expert” knowledge for vegetation indices screening in order to maximize predictability and transferability. The RF analysis was performed in R software (R Development Core Team) [26], using the “randomForest” package [27]. For model validation, 10-fold cross validation was carried out considering the limited number of sample plots for each of the seasons. For cross validation, the “caret” package [28] was used. Further, root mean square error (RMSE) and relative RMSE were calculated from the validation data to quantify the optimal model for seasonal LAI estimation and for further mapping purposes (Figure 3).

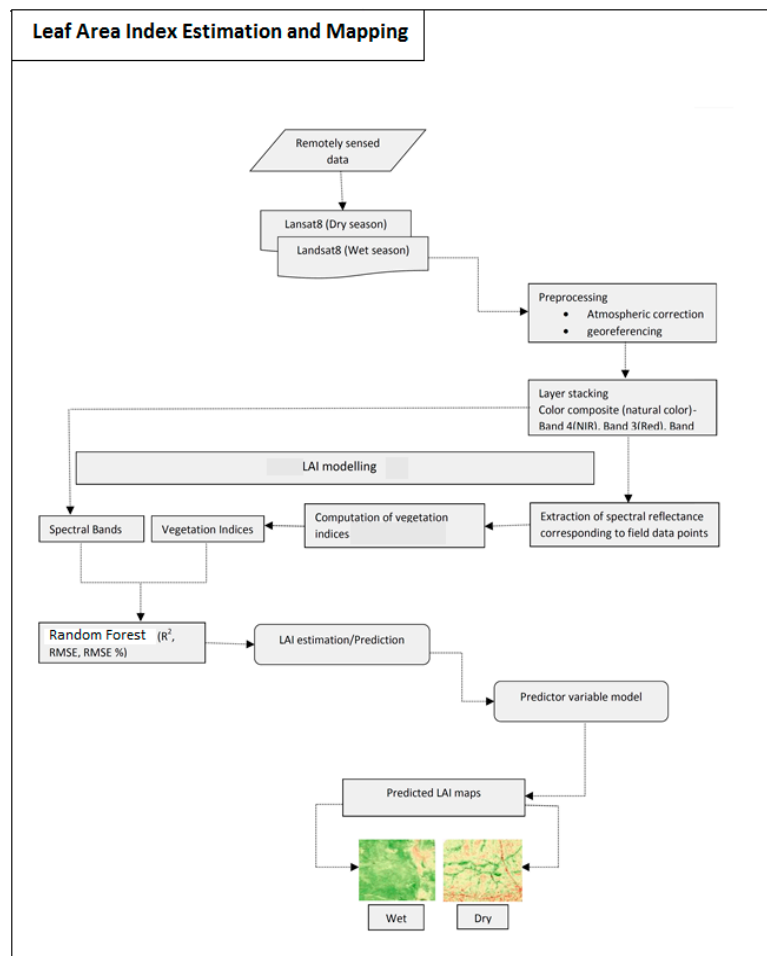


Figure 3. Seasonal LAI computation using is-situ and remotely sensed data.

3. Results

3.1. Statistical Summary of the Measured LAI

Kruger National Park field LAI measurements ranged between 0 and $7.18 \text{ m}^2/\text{m}^2$ ($n = 119$, mean $3.02 \pm 1.18 \text{ m}^2/\text{m}^2$) for the wet season and between 0 and $5 \text{ m}^2/\text{m}^2$ ($n = 74$, mean $2 \pm 1.17 \text{ m}^2/\text{m}^2$) for the dry season, respectively (Table 3). It was evident that the protected area had a greater LAI during the wet season when compared to the dry season demonstrating highest levels of savanna ecosystem productivity during the period. Figure 4 shows the histogram of LAI for dry and wet seasons. It can be observed that the LAI followed a normal distribution curve for both the dry and wet seasons.

Table 3. Random forest (RF) model performance by backward elimination of variables for the wet season. RMSE: root mean square error.

No. of Variables Used	Eliminated Variable (Backward)	R ²	RMSE m ² /m ²	relRMSE%
21	full predictors	0.63	0.70	37.63
20	B3	0.70	0.63	33.82
19	B1	0.69	0.63	33.97
18	B2	0.69	0.62	33.67
17	GVI	0.68	0.63	34.08
16	MSR	0.69	0.63	34.07
15	B4	0.72	0.60	32.48
14	B6	0.68	0.64	34.33
13	MTVI2	0.68	0.64	33.33

Table 3. Cont.

No. of Variables Used	Eliminated Variable (Backward)	R ²	RMSE m ² /m ²	relRMSE%
12	EVI2	0.68	0.63	34.34
11	B7	0.68	0.63	34.14
10	ARVI	0.68	0.63	34.20
9	GNDVI	0.68	0.63	34.23
8	EVI	0.67	0.64	34.57
7	MCARI	0.67	0.64	34.56
6	SR	0.66	0.65	34.92
5	GCI	0.65	0.66	35.36
4	NDVI	0.59	0.70	38.03
3	B5	0.63	0.67	36.19

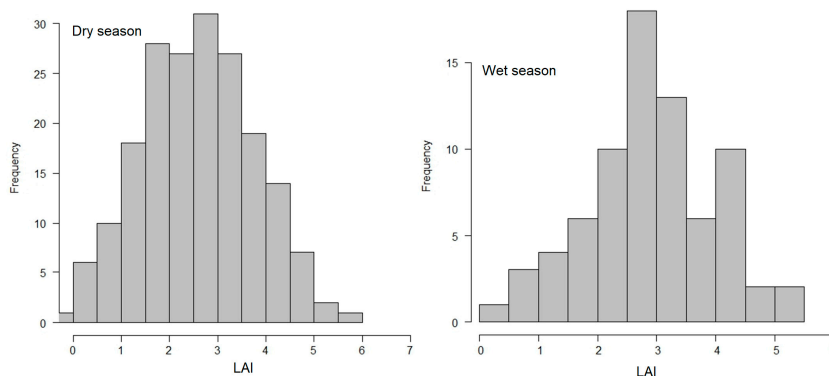


Figure 4. Histogram for predicted LAI for dry season and wet seasons.

3.2. LAI Estimates Using RF Algorithm

The use of RF selected predictor variables resulted in the most accurate LAI estimates for the two seasons. The use of optimal selected variables yielded high coefficient of determination values, ranging from 0.63 to 0.72 (RMSE = 0.70 m²/m², relRMSE = 37.63 m²/m² to RMSE = 0.60, relRMSE = 32.48 m²/m²) for the wet season, whereas for the dry season the range was between 0.62 and 0.63 (RMSE = 0.81 m²/m², relRMSE = 31.07, RMSE = 0.79 m²/m², relRMSE = 29.91) (Table 3). Specifically, the use of the full set of variables without screen compromised the model performance in LAI estimation, yielding an R² of 0.63, RMSE of 0.70 m²/m² and %RMSE of 37.63 for the wet season and the same was observed for the dry season. LAI estimates improved significantly after model screening, demonstrating that other variables were not important in LAI estimation (Tables 3 and 4).

Table 4. RF model performance by backward elimination of variables for dry season data.

No. of Variables Used	Eliminated Variable (Backward)	R ²	RMSE m ² /m ²	relRMSE%
21	full predictors	0.62	0.81	37.63
20	B4	0.61	0.80	33.82
19	EVI2	0.61	0.80	33.97
18	B5	0.61	0.80	33.67
17	MTVI2	0.61	0.80	34.08
16	B3	0.61	0.80	34.07
15	ARVI	0.61	0.80	32.48
14	B7	0.62	0.79	34.33
13	B2	0.62	0.79	33.33
12	MCARI	0.62	0.80	34.34
11	SAVI	0.62	0.80	34.14
10	B1	0.62	0.79	34.20
9	EVI	0.63	0.79	34.23
8	MSR	0.63	0.79	34.57

Table 4. Cont.

No. of Variables Used	Eliminated Variable (Backward)	R ²	RMSE m ² /m ²	relRMSE%
7	NDVI	0.63	0.79	34.56
6	B6	0.62	0.79	34.92
5	SR	0.62	0.79	35.36
4	CRI1	0.61	0.80	38.03
3	PSRI	0.59	0.86	36.19

The accuracy results show that both the dry and wet seasons' LAI could be predicted with reasonable accuracies using multispectral Landsat 8 OLI satellite data. It is also important to note that when the *mtry* increased or decreased, the model accuracy became weak, hence the 500 *mtry* was found to be the most suitable as it resulted in the best LAI model results. Further, the results indicate that Landsat 8 OLI data could more accurately predict LAI during the wet season when compared to the dry season as there would be many bare patches, resulting in spectral mixing and poor model performance. To identify the optimal model, backward elimination of the least important variables generated from the OOB data enhanced the performance of the model for the wet season LAI estimation. However, for the dry season, although there was an improvement in the variance explained by the model and the reduction in the error term, this was minimal. Figure 5 shows the scatter plot between observed LAI and estimated LAI for both seasons. The results indicate a good relationship between observed and estimated LAI, especially for the wet season.

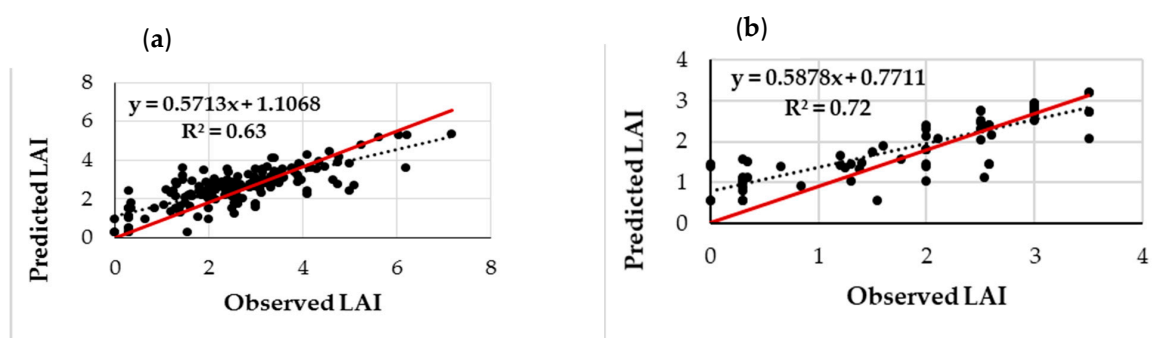


Figure 5. Observed vs. predicted LAI using RF-optimized models: (a) wet season data; (b) dry season data.

3.3. RF Important Variables Selection

CRI1, SAVI, PSRI, B5, NDVI, GCI, SR, MCARI, EVI, GNDVI, ARVI, B7 EVI2, MTVI2 and B6 were RF-model selected as the most important Kruger National Park LAI predictor variables during the wet season, whereas for the dry season, GNDVI, GCI, GVI, PSRI, CRI1, SR, B6, NDVI and MSR were selected (Figure 5a,b). The RF model allows the ranking of the most important variables. Following the ranking process, redundant variables were removed from the modelling of LAI. A total of 15 variables yielded a better result for the wet season data, producing an R² of 0.72, RMSE of 0.60 m²/m² and a relRMSE 32.48, whereas for the dry season LAI data, nine predictor variables were selected, producing an R² of 0.63, RMSE of 0.79 m²/m² and a relRMSE of 34.23 (Figure 6). Overall, the wet season LAI was predicted with a high accuracy when compared to the dry season LAI. However, both LAI predictions were satisfactory and within the acceptable ranges.

3.4. Derived LAI Thematic Maps

The results further showed that there was a significant variation ($\alpha = 0.05$) in LAI between the dry and the wet seasons (Figure 7). It is evident that during the wet season, LAI estimates were high in the Kruger National Park. High LAI estimates were observed in the middle and southern parts of

the park during the wet season. However, the northern parts had low LAI values, demonstrating low productivity in that region during the wet season. In contrast, during the dry season the southern parts of the park were characterized with low LAI estimates and this trend was observed in the middle parts of the park and towards the north. However, the southern parts were more degraded as estimated LAI was around 0.001 m²/m².

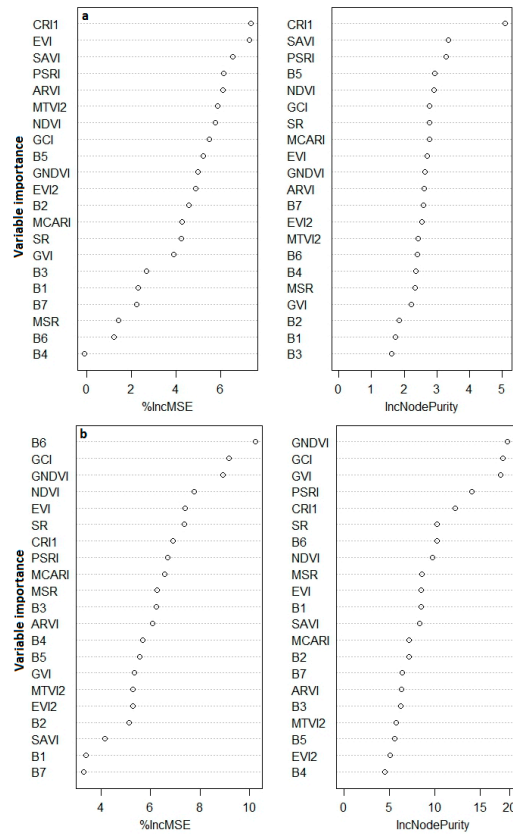


Figure 6. Important variables ranking by RF model (a) wet and (b) dry seasons. %IncMSE: percentage increased mean squared error; IncNodePurity: increased node purity.

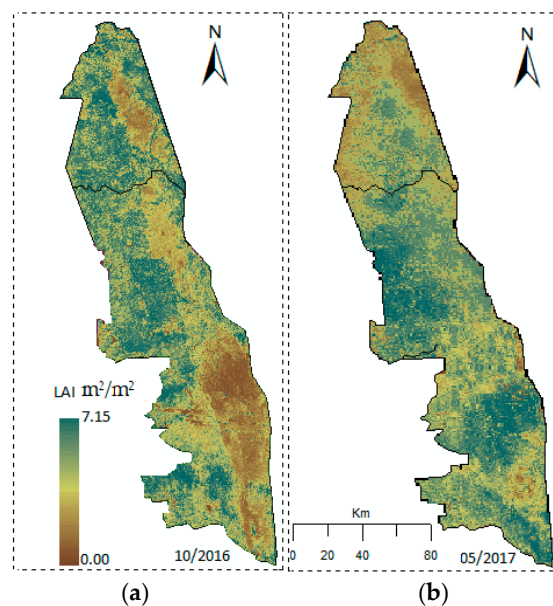


Figure 7. Distribution of LAI in Kruger national park during the (a) dry and (b) wet seasons.

4. Discussion

Kruger National Park, located in South Africa, is one of the most important protected game reserves in sub-Saharan Africa. It is home to a wide range of wild animals and contributes greatly to employment opportunities and economic growth through tourism. According to the South African Department of Environmental Affairs (DeA) and SANParks, 1,659,000 people visited the KNP between 2014 and 2015 financial years. This is a clear indication of how important protected areas in tropical savanna ecosystems are to the economy through tourism. It is therefore imperative to ensure that ecosystem productivity in these areas is routinely monitored and conserved from degradation or overgrazing. This understanding is critical as it provides park managers with the necessary baseline information about forage distribution and productivity dynamics within the park, which is fundamental in planning and management. In this study, we assessed the spatio-temporal dynamics of LAI for the dry and wet seasons, as a proxy for rangeland condition and productivity in the Kruger National Park, South Africa. Vegetation LAI is indicative of vegetation productivity, and its characterization using satellite data at landscape scale plays a critical role in determining the ability of the reserve in providing forage for wildlife.

4.1. Variations in LAI between Wet and Dry Season

The results demonstrated that the variations in LAI between the wet and dry seasons could be clearly depicted using Landsat 8 data. The mean estimated LAI values were slightly lower during the dry season ($1.86 \text{ m}^2/\text{m}^2$) when compared to the wet season ($2.61 \text{ m}^2/\text{m}^2$). Nevertheless, the relationship between LAI and satellite-derived spectral bands and vegetation indices were better-explained (72%) for the wet season when compared to the dry season. Although some of the plots showed predicted LAI values that were distinctly higher than the observed and vice-versa, the error term was highest for the extreme values, which can be explained by prevailing heterogeneous shrub vegetation in the study site.

In addition, the study produced medium-resolution maps depicting the spatio-temporal LAI estimates using machine learning, RF regression. The relationship between spectrally derived vegetation indices and LAI estimates obtained from field LAI measured data for the two time periods was within the acceptable ranges. A comparative analysis of dry and wet seasons for LAI estimated, with selected vegetation indices (VIs) depicted a better result for the wet season. Furthermore, the RF optimization enhanced the model performance ($R^2 = 0.72$, $\text{RMSE} = 0.60 \text{ m}^2/\text{m}^2$). Most notably, the RF model tended to under-predict high LAI values and over-predict low LAI values. This was observed for both the dry and wet seasons. This has been found to be a common phenomenon in RF regression resulting from averaging the prediction from each tree used in the RF model [22,29–31].

Observed LAI estimation accuracies can be associated with the RF regression algorithm. This is because the model has the ability to interrogate, rank and screen variables based on their importance, and this has been found to help improve model accuracy. Literature shows that the inclusion of less-important variables in modelling results in the convergence and instability of models or introduces random errors, due to noise from predictor variables without any relation to the response variable [31–34]. Thus, in this study, the tuning of *ntree* and *mtry* parameters to build the model further enhanced the model performance in estimating LAI for the wet and dry seasons. Our findings are in line with studies conducted elsewhere [31–34]. A study by Grömping [34] showed that the choice of *mtry* in the RF model could affect the ranking of predictor variables. For our study, the RF model identified the smallest subset of the variables that led to a parsimonious model by reducing the reductant variable effect to fifteen and nine input variables for LAI estimation in the wet and dry seasons, respectively. Similar model performances were reported in References [15,17], whose work demonstrated that key vegetation biophysical characteristics could be predicted with high accuracy when using model selected important variables.

Although not tested in this study, the performance of Landsat 8 OLI satellite images in estimating LAI can be attributed to the unique sensor design. For instance, Landsat 8 OLI makes

use of numerous elongated sets of detectors for each waveband capable of a detailed scan of the surface along-track. The along-track design augments the sensitivity of the sensor to most critical vegetation biophysical metrics. Furthermore, the presence of a refined spectral range of particular wavebands (e.g., near-infrared) plays a fundamental function in boosting the detection of subtle grassland biophysical and biochemical characteristics, whereas the enhanced image radiometric resolution (12 bits) permits the precise detection of various vegetation conditions [35–37]. These results demonstrate the unique potential of the Landsat 8 multi-spectral sensor in vegetation or rangeland mapping and monitoring in tropical savanna ecosystems.

4.2. Performance of Landsat 8 Variables in Characterizing Seasonal LAI

The RF generated variable important results identified CRI1 (carotenoids reflectance index 1) as the most important variable for the wet season. Carotenoids function as the light absorption processes in plants and is related to high chlorophyll concentration. Thus, for the wet season data, CRI1 was ranked as most important predictor variables. Similarly, SAVI was identified as the second-most important variable for predicting LAI in tropical savanna ecosystems [38,39]. For the dry season, the GNDVI was identified as the most important variable. Since chlorophyll content is low during the dry season, the green band tends to be more sensitive to chlorophyll than the red channel [38,40–42]. The results indicated that visible bands' reflectance sensitivity to LAI varied seasonally.

Previous studies [43,44] have highlighted a strong relationship between LAI and various vegetation indices, mainly for the most frequently used NDVI and SAVI. These indices enhance the contrast between the spectral differences between vegetation and soil, but they are sensitive to the optical properties of the soil background and also experience saturation problems when LAI is high ($6 \text{ m}^2/\text{m}^2$), depending on the vegetation types [38,45]. Thus, in this study, we tried not to limit the important role of VIs in explaining the leaf characteristics, as we introduced more VIs.

4.3. The Implications of Seasonal LAI Estimations for Reserve

Accurate estimation of LAI in tropical savanna rangelands provides a critical input dataset required for ecological modelling and the accurate quantification of ecosystem productivity using the Landsat 8 OLI. Understanding current dynamics and potential changes in ecosystem productivity (quality and quantity) is critical for sustainable wildlife and livestock production. A number of studies [46–48] have used LAI to model vegetation cover, growth, productivity and the effects of disturbances such as climate change, drought and defoliation on vegetation communities. The study by Ramoelo et al. [3] also emphasized the importance of an appropriate algorithm for identifying the optimal remote sensing variables to improve the LAI estimation accuracy. The LAI of grass species might be related to the solar energy and dry biomass production, and should be included in modelling rangeland productivity in future studies. The services of other freely-available broadband multispectral satellites (e.g., Sentinel-2) with better estimation accuracy might also have a positive effect in terms of accurately monitoring LAI across grass species functional types, especially considering the current demand for vegetation information [7]. The demand for vegetation information—particularly in endangered biomes such as tropical savanna—has been on the rise given the need to improve the management and conservation of these valuable ecosystems.

5. Conclusions

Our study has shown that:

1. With its improved sensing characteristics, the Landsat 8 OLI has the ability to explain and predict the spatio-temporal dynamics in LAI in tropical savanna rangelands with acceptable accuracy.
2. LAI could be estimated with high accuracy during the wet season when compared to the dry season using RF model—a previously challenging task with traditional linear techniques.

- The derived KNP LAI thematic maps indicate that forage productivity varied significantly ($\alpha = 0.05$) between the wet and dry seasons, hence the need for monitoring wildlife movements and grazing patterns so that degradation can be minimal.

For effective conservation of tropical savanna rangelands, including Kruger National Park, sustainable land management practices and coordinated research and monitoring of wildlife grazing patterns and rangeland productivity is required. Our results indicate that the tropical savanna rangelands are likely to have less forage quantity during the dry season. Unsustainable grazing patterns may cause land degradation, especially if limited rain is received during the wet season. However, we recommend further research in tropical savanna rangeland productivity monitoring and assessment across different land management units. The inclusion of other variables like rainfall patterns and plant diseases is also crucial in understanding these ecosystems.

Author Contributions: T.D. conceptualized idea and wrote the manuscript; S.P. analysed the data; C.S. collected data and wrote the paper; A.R. conceptualized idea and guided the write-up, analysis, and editing; D.M. edited and gave scientific comments and suggestions; and T.D. edited the manuscript and contributed to packaging the idea.

Funding: This research received no external funding.

Acknowledgments: We thank Kruger National Park authorities for allowing us to use their premises to conduct this study. We would like to thank the Editors and reviewers from the *Remote Sensing* MDPI Special Issue “Leaf Area Index (LAI) Retrieval Using Remote Sensing” for handling and the constructive comments and suggestions that helped improve the quality of the manuscript.

Conflicts of Interest: The authors declare no conflict of interest.

References

- Munyati, C.; Shaker, P.; Phasha, M.G. Using remotely sensed imagery to monitor savanna rangeland deterioration through woody plant proliferation: A case study from communal and biodiversity conservation rangeland sites in Mokopane, South Africa. *Environ. Monit. Assess.* **2011**, *176*, 293–311. [[CrossRef](#)] [[PubMed](#)]
- Palmer, A.R.; Samuels, I.; Cupido, C.; Finca, A.; Kangombe, W.F.; Yunusa, I.A.; Vetter, S.; Mapaire, I. Aboveground biomass production of a semi-arid southern African savanna: Towards a new model. *Afr. J. Range Forage Sci.* **2016**, *33*, 43–51. [[CrossRef](#)]
- Ramoelo, A.; Cho, M.A.; Mathieu, R.S.; Skidmore, A.; Schlerf, M.; Heitkönig, I. Estimating grass nutrients and biomass as an indicator of rangeland (forage) quality and quantity using remote sensing in Savanna ecosystems. In Proceedings of the 9th International Conference of the African Association of Remote Sensing and the Environment (AARSE), El-Jadida, Morocco, 28 October–2 November 2012.
- Department of Environmental Affairs and Tourism. *White Paper on the Conservation and Sustainable Use of South Africa’s Biological Diversity: Draft for Discussion*; Department of Environmental Affairs and Tourism: Pretoria, South Africa, 1997; Available online: <https://searchworks.stanford.edu/view/4445125> (accessed on 13 November 2018).
- Alkemade, R.; Reid, R.S.; van den Berg, M.; de Leeuw, J.; Jeuken, M. Assessing the impacts of livestock production on biodiversity in rangeland ecosystems. *Proc. Natl. Acad. Sci. USA* **2013**, *110*, 20900–20905. [[CrossRef](#)] [[PubMed](#)]
- Zheng, G.; Moskal, L.M. Retrieving leaf area index (LAI) using remote sensing: Theories, methods and sensors. *Sensors* **2009**, *9*, 2719–2745. [[CrossRef](#)] [[PubMed](#)]
- Dube, T.; Mutanga, O. Evaluating the utility of the medium-spatial resolution Landsat 8 multispectral sensor in quantifying aboveground biomass in uMgeni catchment, South Africa. *ISPRS J. Photogramm. Remote Sens.* **2015**, *101*, 36–46. [[CrossRef](#)]
- Rouse, J.W., Jr. *Monitoring the Vernal Advancement and Retrogradation (Green Wave Effect) of Natural Vegetation*; NASA/GSFC Final Report; Texas A and M University, Remote Sensing Center: College Station, TX, USA, 1974.
- Jordan, C.F. Derivation of leaf-area index from quality of light on the forest floor. *Ecology* **1969**, *50*, 663–666. [[CrossRef](#)]
- Huete, A.R. A soil-adjusted vegetation index (SAVI). *Remote Sens. Environ.* **1988**, *25*, 295–309. [[CrossRef](#)]

11. Huete, A.; Didan, K.; Miura, T.; Rodriguez, E.P.; Gao, X.; Ferreira, L.G. Overview of the Radiometric and Biophysical Performance of the MODIS Vegetation Indices. *Remote Sens. Environ.* **2002**, *83*, 195–213. [[CrossRef](#)]
12. Merzlyak, M.N.; Gitelson, A.A.; Chivkunova, O.B.; Rakitin, V.Y. Non-destructive Optical Detection of Pigment Changes During Leaf Senescence and Fruit Ripening. *Physiol. Plant.* **1999**, *106*, 135–141. [[CrossRef](#)]
13. Gitelson, A.A.; Zur, Y.; Chivkunova, O.B.; Merzlyak, M.N. Assessing Carotenoid Content in Plant Leaves with Reflectance Spectroscopy. *Photochem. Photobiol.* **2002**, *75*, 272–281. [[CrossRef](#)]
14. Kauth, R.; Thomas, G.S. The tasseled cap—A graphic description of the spectral-temporal development of agricultural crops as seen by Landsat. In *LARS Symposia*; Purdue University: West Lafayette, Indiana, 1976; p. 159. Available online: http://docs.lib.purdue.edu/lars_symp (accessed on 12 October 2018).
15. Gitelson, A.; Merzlyak, M.N. Remote Sensing of Chlorophyll Concentration in Higher Plant Leaves. *Adv. Space Res.* **1998**, *22*, 689–692. [[CrossRef](#)]
16. Gitelson, A.; Gritz, Y.; Merzlyak, M.N. Relationships Between Leaf Chlorophyll Content and Spectral Reflectance and Algorithms for Non-Destructive Chlorophyll Assessment in Higher Plant Leaves. *J. Plant Physiol.* **2003**, *160*, 271–282. [[CrossRef](#)] [[PubMed](#)]
17. Qi, J.; Chehbouni, A.; Huete, A.R.; Kerr, Y.H.; Sorooshian, S. A modified soil adjusted vegetation index. *Remote Sens. Environ.* **1994**, *48*, 119–126. [[CrossRef](#)]
18. Kaufman, Y.; Tanre, D. Atmospherically Resistant Vegetation Index (ARVI) for EOS-MODIS. *IEEE Trans. Geosci. Remote Sens.* **1992**, *30*, 261–270. [[CrossRef](#)]
19. Daughtry, C.S.T.; Walthall, C.L.; Kim, M.S.; De Colstoun, E.B.; McMurtrey, J.E., III. Estimating Corn Leaf Chlorophyll Concentration from Leaf and Canopy Reflectance. *Remote Sens Environ.* **2000**, *74*, 229–239. [[CrossRef](#)]
20. Haboudane, D.; Miller, J.R.; Pattey, E.; Zarco-Tejada, P.J.; Strachan, I.B. Hyperspectral Vegetation Indices and Novel Algorithms for Predicting Green LAI of Crop Canopies: Modeling and Validation in the Context of Precision Agriculture. *Remote Sens. Environ.* **2004**, *90*, 337–352. [[CrossRef](#)]
21. Pandit, S.; Tsuyuki, S.; Dube, T. Estimating above-ground biomass in sub-tropical buffer zone community Forests, Nepal, using Sentinel-2 data. *Remote Sens.* **2018**, *10*, 601. [[CrossRef](#)]
22. Jeong, J.H.; Resop, J.P.; Mueller, N.D.; Fleisher, D.H.; Yun, K.; Butler, E.E.; Timlin, D.J.; Shim, K.M.; Gerber, J.S.; Reddy, V.R.; et al. Random Forests for Global and Regional Crop Yield Predictions. *PLoS ONE* **2016**, *11*, e0156571. [[CrossRef](#)]
23. Breiman, L. Random forests. *Mach. Learn.* **2001**, *45*, 5–32. [[CrossRef](#)]
24. Dube, T.; Mutanga, O.; Elhadi, A.; Ismail, R. Intra-and-inter species biomass prediction in a plantation forest: Testing the utility of high spatial resolution space borne multispectral RapidEye sensor and advance machine learning algorithms. *Remote Sens.* **2014**, *14*, 15348–15370. [[CrossRef](#)]
25. Scornet, E.; Biau, G.; Vert, J.P. Consistency of random forests. *Ann. Stat.* **2015**, *43*, 1716–1741. [[CrossRef](#)]
26. R Development Core Team. R: A Language and Environment for Statistical Computing. Available online: www.R-project.org (accessed on 12 October 2018).
27. Liaw, A.; Matthew, W. Classification and regression by randomforest. *R News* **2002**, *2*, 18–22.
28. Kuhn, M. Building Predictive Models in R Using the caret Package. *J. Stat. Softw.* **2008**, *28*, 1–26. [[CrossRef](#)]
29. Horning, N. Random Forests: An algorithm for image classification and generation of continuous fields data sets. In Proceedings of the International Conference on Geoinformatics for Spatial Infrastructure Development in Earth and Allied Sciences, Osaka, Japan, 22 October 2010; Volume 911.
30. Adam, E.M.; Mutanga, O.; Abdel-Rahman, E.M.; Ismail, R. Estimating standing biomass in papyrus (*Cyperus papyrus* L.) swamp: Exploratory of in situ hyperspectral indices and random forest regression. *Int. J. Remote Sens.* **2014**, *35*, 693–714. [[CrossRef](#)]
31. Wong, V.C.W. Optimizing Digital Aerial Photogrammetry for Forestry Applications in Tropical Montane Forest Environment. Ph.D. Thesis, University of Tokyo, Tokyo, Japan, 2016.
32. Genuer, R.; Poggi, J.M.; Tuleau-Malot, C. Variable selection using random forests. *Pattern Recognit. Lett.* **2010**, *31*, 2225–2236. [[CrossRef](#)]
33. Oshiro, T.M.; Perez, P.S.; Baranauskas, J.A. How many trees in a random forest? In *International Workshop on Machine Learning and Data Mining in Pattern Recognition*; Springer: Berlin/Heidelberg, Germany, 2012; pp. 154–168. [[CrossRef](#)]
34. Biau, G.; Scornet, E. A random forest guided tour. *Test* **2016**, *25*, 197–227. [[CrossRef](#)]

35. Grömping, U. Variable importance assessment in regression: Linear regression versus random forest. *Am. Stat.* **2009**, *63*, 308–319. [[CrossRef](#)]
36. Nackaerts, K.; Coppin, P.; Muys, B.; Hermy, M. Sampling methodology for LAI measurements with LAI-2000 in small forest stands. *Agric. For. Meteorol.* **2000**, *101*, 247–250. [[CrossRef](#)]
37. Manssour, K.M.Y. Rangeland Degradation Assessment Using Remote Sensing and Vegetation Species. Ph.D. Thesis, University of KwaZulu-Natal, Pietermaritzburg, South Africa, 2011. Available online: <http://hdl.handle.net/10413/8583> (accessed on 12 October 2018).
38. Bulcock, H.; Jewitt, G. Spatial mapping of leaf area index using hyperspectral remote sensing for hydrological applications with a particular focus on canopy interception. *Hydrol. Earth Syst. Sci.* **2010**, *14*, 383–392. [[CrossRef](#)]
39. Baret, F.; Guyot, G. Potentials and limits of vegetation indices for LAI and APAR assessment. *Remote Sens. Environ.* **1991**, *35*, 161–173. [[CrossRef](#)]
40. Papadavid, G.C.; Hadjimitsis, D.G.; Toullos, L.; Michaelides, S. Mapping potato crop height and leaf area index through vegetation indices using remote sensing in Cyprus. *J. Appl. Remote Sens.* **2011**, *5*, 053526. [[CrossRef](#)]
41. Yoder, B.J.; Waring, R.H. The normalized vegetation index of small douglas-fir canopies with varying chlorophyll concentration. *Remote Sens. Environ.* **1994**, *49*, 81–91. [[CrossRef](#)]
42. Gitelson, A.A.; Stark, R.; Grits, U.; Rundquist, D.; Kaufman, Y.; Derry, D. Vegetation and soil lines in visible spectral space: A concept and technique for remote estimation of vegetation fraction. *Int. J. Remote Sens.* **2002**, *23*, 2537–2562. [[CrossRef](#)]
43. Wang, F.M.; Huang, J.F.; Tang, Y.L.; Wang, X.Z. New vegetation index and its application in estimating leaf area index of rice. *Rice Sci.* **2007**, *14*, 195–203. [[CrossRef](#)]
44. Zhang, C. The evaluation of broadband vegetation indices on monitoring Northern mixed grassland. *Prairie Perspect.* **2005**, *8*, 23–36. Available online: <http://pcag.uwinnipeg.ca/Prairie-Perspectives/PP-Vol08/Zhang.pdf> (accessed on 12 November 2018).
45. He, Y.; Guo, X. Leaf Area Index estimation using remotely sensed data in mixed grassland ecosystem. *Prairie Perspect.* **2006**, *9*, 105–117. Available online: <http://hdl.handle.net/1807/69335> (accessed on 15 October 2018).
46. Wanjura, D.F.; Hatfield, J.L. Sensitivity of spectral vegetative indices to crop biomass. *Trans. ASAE* **1987**, *30*, 0810–0816. [[CrossRef](#)]
47. Gray, J.; Song, C. Mapping leaf area index using spatial, spectral, and temporal information from multiple sensors. *Remote Sens. Environ.* **2012**, *119*, 173–183. [[CrossRef](#)]
48. Shen, L.; Li, Z.; Guo, X. Remote sensing of leaf area index (LAI) and a spatiotemporally parameterized model for mixed grasslands. *Int. J. Appl. Sci. Technol.* **2014**, *4*. Available online: http://ijastnet.com/journals/Vol_4_No_1_January_2014/5.pdf (accessed on 13 January 2019).
49. Rutherford, M.; Powrie, L. Impacts of heavy grazing on plant species richness: A comparison across rangeland biomes of South Africa. *S. Afr. J. Bot.* **2013**, *87*, 146–156. [[CrossRef](#)]



© 2019 by the authors. Licensee MDPI, Basel, Switzerland. This article is an open access article distributed under the terms and conditions of the Creative Commons Attribution (CC BY) license (<http://creativecommons.org/licenses/by/4.0/>).